Thermodynamic Modeling of the Drowning-Out Crystallization Process for LiOH and CHLiO$_2$

Raquel González [1], Yahaira Barrueto [2,3] and Yecid P. Jiménez [1,4,*]

1. Departamento de Ingeniería Química y Procesos de Minerales, Facultad de Ingeniería, Universidad de Antofagasta, Av. Angamos 601, Antofagasta 1240000, Chile; raquel.gonzalez.roblero@ua.cl
2. Departamento de Ingeniería Metalúrgica y Materiales, Universidad Técnica Federico Santa María, Valparaíso 2340000, Chile; yahaira.barrueto@usm.cl
3. Sustainable Minerals Institute–International Centre of Excellence Chile (SMI-ICE-Chile), The University of Queensland, Australia, Av. Apoquindo 2929, 3rd Floor Office 301, Santiago 7550000, Chile
4. Centro de Economía Circular en Procesos Industriales (CECPI), Facultad de Ingeniería, Universidad de Antofagasta, Av. Angamos 601, Antofagasta 1240000, Chile
* Correspondence: yecid.jimenez@uantof.cl

Abstract: This study focuses on the thermodynamic modeling of the crystallization by the drowning process for two lithium salts: lithium hydroxide (LiOH) and lithium formate (CHLiO$_2$). The modeling involves utilizing thermodynamic properties, such as the activity, osmotic, and solubility coefficients, within the ternary systems of LiOH + cosolvent + water and CHLiO$_2$ + cosolvent + water, as well as their respective binary constituent systems. Ethanol is chosen as the cosolvent for both salts, facilitating a comparative analysis. Given the limited availability of thermodynamic data for lithium formate with different cosolvents, the study aims to address this gap. The modified Pitzer model was employed for the modeling process, where the parameters were successfully obtained for both systems, with a deviation of less than 1%. Additionally, the mass and energy balance for the drowning-out crystallization process of both salts was performed.

Keywords: crystallization; lithium salts; thermodynamic properties; modified Pitzer model

1. Introduction

Nonmetallic mining in Chile has always been of worldwide interest thanks to the country's geology and climate, where one of the most commercialized nonmetallic products are lithium salts, particularly lithium carbonate and lithium hydroxide. Lithium carbonate is the most industrially used compound worldwide; this is because it is used to obtain lithium hydroxide monohydrate, whose thermodynamic properties are of great importance for geochemical processes, such as brine formation [1,2]. As for lithium carbonate, it accounts for approximately 71% of industrial use, as its purification process is simple, and it is used for the conversion of organic and inorganic lithium salts [3]. Although lithium has great utilities and is a natural resource with great global and national presence, it is still a subject of research since there are many lithium compounds with few studies, such as lithium formate (CHLiO$_2$).

Drowning crystallization is generally used to separate components that are difficult to distill. This type of crystallization is widely used in the separation of heat-sensitive components because crystallization occurs near room temperature and increases the yield of components that have a solubility that varies relatively little with temperature [4]. The drowning-out crystallization of highly water-soluble ionic solids can be induced by the addition of water-miscible organic antisolvents, such as monovalent alcohols. These antisolvents can modify the structure, properties, and behavior of electrolyte solutions, causing changes in the mobility and solvation of ions. The mixing of solvents has a significant effect on the dielectric constant of the solution, since a decrease in the dielectric

constant in mixtures of water and solvent is linked to an increase in the electrostatic interaction between ions of opposite charge, which favors the formation of insoluble ionic species [5,6]. For each value of electrical constant, there is a critical distance for which the electrostatic interaction energy is equal to the average kinetic energy of the charged ions. Below the value of the critical distance, the ions cannot be separated by agitation, and therefore ionic pairs are formed. It is because of the abovementioned that it is concluded that the addition of some organic antisolvent to an aqueous solution of an ionic salt leads to an increase in the ionic cohesion forces, and thus precipitation will occur [7].

The Pitzer model [8] has been used for solubility prediction and correlation in systems containing one or more salts in a single solvent [9,10]. However, this original form of the model is not successfully applied for electrolyte solutions with mixed solvents [11]. To extend the application of this model, Wu et al. [12] proposed a modified Pitzer model for the liquid–liquid equilibrium prediction of polymer + salt + water systems; this modified model was successfully applied [13]. This modified Pitzer model considers the existence of short- and long-range interactions described by binary and ternary parameters. The modified model has been applied to determine the different thermodynamic properties of electrolyte solutions [14–16]. The generated parameters are fundamental to describe, understand, and project the behavior of associated multicomponent systems [17,18].

Taboada et al. [19] studied the crystallization process by the drowning of the LiOH + ethanol + water system using the graphical method at 298.15 K, i.e., no thermodynamic modeling was performed. Another related work is that of Graber et al. [20], who studied the behavior of LiOH·H$_2$O crystals obtained by evaporation and drowning, although this work included thermodynamic modeling with the NRTL model; some doubts have arisen about the procedure used, since the reported Kps equation is in a molar scale, and the model parameters and the NRTL model itself works in the mole fraction scale.

This study aims to model the drowning crystallization processes for two lithium salts, lithium hydroxide (LiOH) and lithium formate (CHLiO$_2$), using the modified Pitzer model. The realization of this study will complement the information already published in the literature, providing a contribution to the study of lithium salts and especially considering lithium formate (CHLiO$_2$), which will mean a great contribution for future studies around nonmetallic mining.

2. Thermodynamic Framework

2.1. Solubility Product

The solubility product expression for anhydrous univalent salts (K$_{sp}$) is represented by Equation (1), where x_2 represents the saturation (solubility) mole fraction and $\gamma_\pm$ is the average ionic activity coefficient of the salt. To calculate $\gamma_\pm$, the modified Pitzer model originally reported for mixtures involving water, polymer, and electrolyte is used:

$$K_{sp} = x_2^2 \, \gamma_\pm^2 \tag{1}$$

2.2. Modified Pitzer Model

According to the modified Pitzer model [8], the activity coefficients, γ, may be written as described by Equation (2), in which the superscripts *LR* and *SR* stand for the long-range and short-range contributions of the species *i*, respectively.

$$\ln \gamma_i = \ln\gamma_i{}^{LR} + \ln\gamma_i{}^{SR} \tag{2}$$

For the electrolytes 1:1, the long-range contribution is defined by Equation (3), and for the nonionic components, by Equation (4), where V_i is the molar volume of the pure nonionic species *i* and *d* represents the mixed-solvent density.

$$\ln\gamma_\pm^{LR} = \frac{AI^{\frac{1}{2}}}{\left(1 + bI^{\frac{1}{2}}\right)} \tag{3}$$

$$\ln\gamma_i^{LR} = \frac{2AV_id}{b^3}\left[1 + bI^{\frac{1}{2}} - \left(1 + bI^{\frac{1}{2}}\right)^{-1} - 2\ln\left(1 + bI^{\frac{1}{2}}\right)\right] \tag{4}$$

The ionic strength (I), expressed by Equation (5), depends on the concentration (molality) of species j (m') and its charge (Z).

$$I = 0.5\sum_{j\neq w}^{N} m'_j Z_j^2 \tag{5}$$

A and b are Debye–Hückel constants, based on a value of 4 Å for a; these parameters are calculated using Equations (6) and (7) below:

$$A = 1.327757 * 10^5 \frac{d^{0.5}}{(DT)^{1.5}} \tag{6}$$

$$b = 6.359696 \frac{d^{0.5}}{(DT)^{0.5}} \tag{7}$$

The properties of the mixed solvent D and d are empirically calculated using Equations (8) and (9), where ϕ'_i is the free salt volume fraction of the nonionic species i in the liquid phase. Table 1 shows the physical properties of ethanol and water used to calculate the Debye–Hückel constants A and b.

$$D = \sum \phi'_i D_i \tag{8}$$

$$d = \sum \phi'_i d_i \tag{9}$$

Table 1. Dielectric constant (D_i), density (d_i), and molar volume (V_i) of pure substances used for the calculation of A and b, and the number of segments, r_i, at 298.15 K.

Di		di (kg/m³)		Vi (m³/mol)		PM (g/mol)		r_i	
H₂O	Ethanol	H₂O	Ethanol	H₂O	Ethanol	H₂O	Ethanol	H₂O	Ethanol
78.3040	24.2000	997.0449	785.1000	1.81×10^{-5}	5.87×10^{-5}	18.0200	46.0700	1	1

[21–24].

The short-range contributions for the three components may be written as presented by Equations (10)–(12):

$$ln\gamma_1^{SR} = 2B_{11}r_1^2m_1 + B_{12}r_1m_2 - \frac{M_1}{1000}\frac{n_w}{n_s}I\left(B'_{12}r_1m_1m_2 + 2v_cv_aB'_{22}m_2^2\right) + 3C_{111}r_1^3m_1^2 + 2C_{112}r_1^2m_1m_2 + C_{122}r_1m_2^2 \tag{10}$$

$$\ln\gamma_\pm^{SR} = \left(\frac{1}{v}\right)\left[B_{12}r_1m_1 + 4v_cv_aB_{22}m_2 + I\left(B'_{12}r_1m_1 + 2v_cv_aB'_{22}m_2\right) + C_{112}r_1^2m_1^2 + 2C_{122}r_1m_1m_2 + 2(v_cv_a)^{\frac{3}{2}}C_{222}^\gamma m_2^2\right] \tag{11}$$

$$ln\gamma_3^{SR} = -\frac{M_3}{1000}[B_{11}r_1^2m_1^2 + \left(B_{12} + \frac{n_w}{n_s}IB'_{12}\right)r_1m_1m_2 + 2v_cv_a\left(B_{22} + \frac{n_w}{n_s}IB'_{22}\right)m_2^2 + 2C_{111}r_1^3m_1^3 + 2C_{112}r_1^2m_1^2m_2$$
$$+ 2C_{122}r_1m_1m_2^2 + 2(v_cv_a)^{\frac{3}{2}}C_{222}^\phi m_2^3] \tag{12}$$

where the parameters involved are defined in Supplementary Material (Equations (S1)–(S10)).

3. Bibliographic Background

3.1. Lithium Hydroxide

The study utilized data from Taboada et al. [25] to examine solubility and density variations in binary (lithium hydroxide and water) and ternary (lithium hydroxide, ethanol, and water) systems across different temperatures. Additionally, molality calculations were based on data from another study by Taboada et al. [26], although recorded at a single temperature (298.15 K). Osmotic coefficient information, including viscosity, density, refractive index, and electrical conductivity at 298.15 K, was sourced from Nasirzadeh et al. [1]. Data

on osmotic coefficients, and the activity at various molalities and temperatures, were also obtained from studies by Robinson and Stokes [27] and Hamer and Yung [28].

3.2. Lithium Formate

Data reported by Carton et al. [29], where the solubility (s%) and density (kg/m^3) data are available at different temperatures, were compiled. For osmotic coefficients and activity data, the article by Kreis and Wood [30] was used, where data at different molalities are presented.

3.3. Data Analysis

The osmotic coefficient data from Robinson and Stokes [27] and Hammer [28] exhibit a high degree of similarity, suggesting good reliability. Although the data from Nasirzadeh et al. [1] show a lower similarity to the former two, they follow a similar trend, especially in the range of approximately 2 molal to 5 molal. The disparity in Nasirzadeh's data may be attributed to differences in experimental procedures. Hammer's study involves correcting literature data, including that of Robinson and Stokes, aiming for thermodynamic consistency and expected similarity. In contrast, Nasirzadeh's data were experimentally obtained due to a lack of comprehensive temperature-dependent studies in the existing literature for lithium hydroxide. Figure 1 illustrates a comparison of the three mentioned datasets.
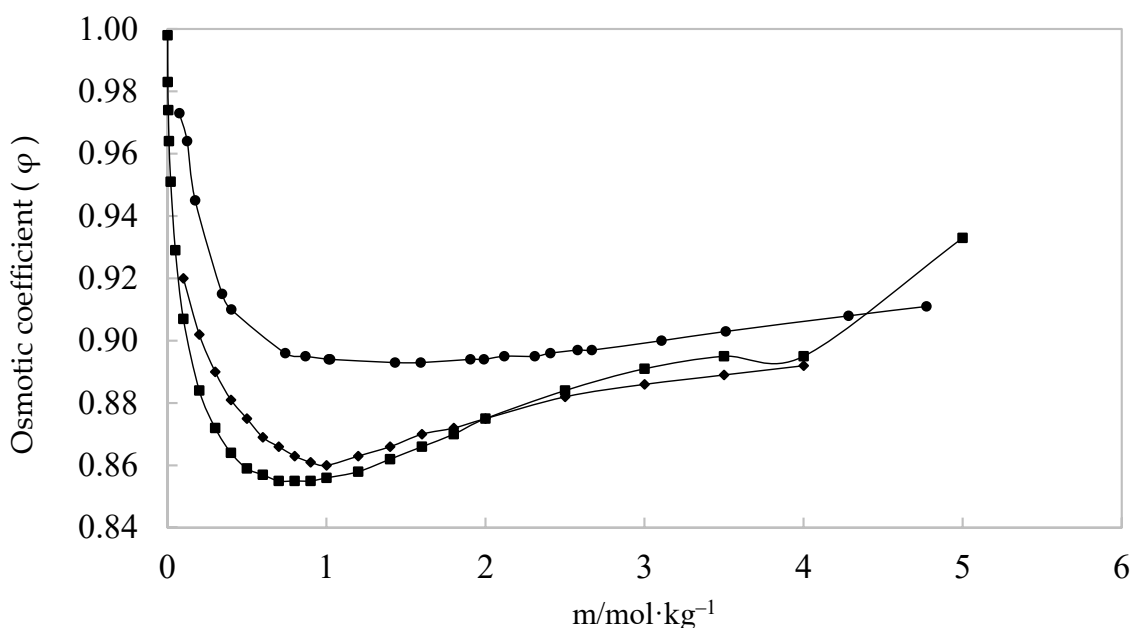

Figure 1. Comparison of osmotic coefficient data for the LiOH + H$_2$O system at 298.15 K. [1] –●–, [27] –♦–, and [28] –■–.

As in the previous case, the activity coefficient data of Robinson and stokes [27] with those of Hammer [28] have a fairly marked similarity, which differs from those of Nasirzadeh et al. [1], being more notable in this case. For the three studies considered at 298.15 K, it can be said that the data are relatively consistent, as they follow the same trend, although they differ from each other, as shown in Figure 2.
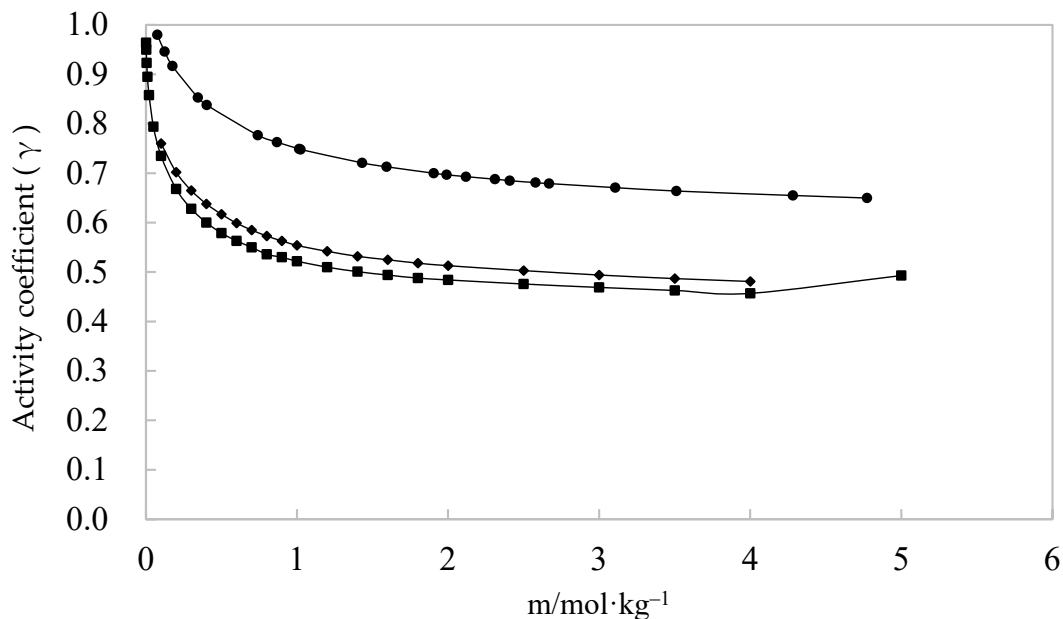
Figure 2. Comparison of activity coefficient data for the LiOH + H$_2$O system at 298.15 K. [1] –●–, [27] –♦–, and [28] –■–.

Limited data are available for the osmotic coefficient and activity in lithium formate, particularly in the binary system, raising concerns about the potential bias in the modeling due to the narrow molal concentration range. The solubility data for the lithium formate ternary system are more extensive, primarily reported by a single author and depicted in Figure 3. A notable trend in solubility is observed at low alcohol concentrations, where higher temperatures correspond to increased solubility. However, as the ethanol concentration rises, the temperature's impact on solubility diminishes, leading to closely spaced isotherms. This proximity poses a potential challenge in the modeling process, considering experimental uncertainties.
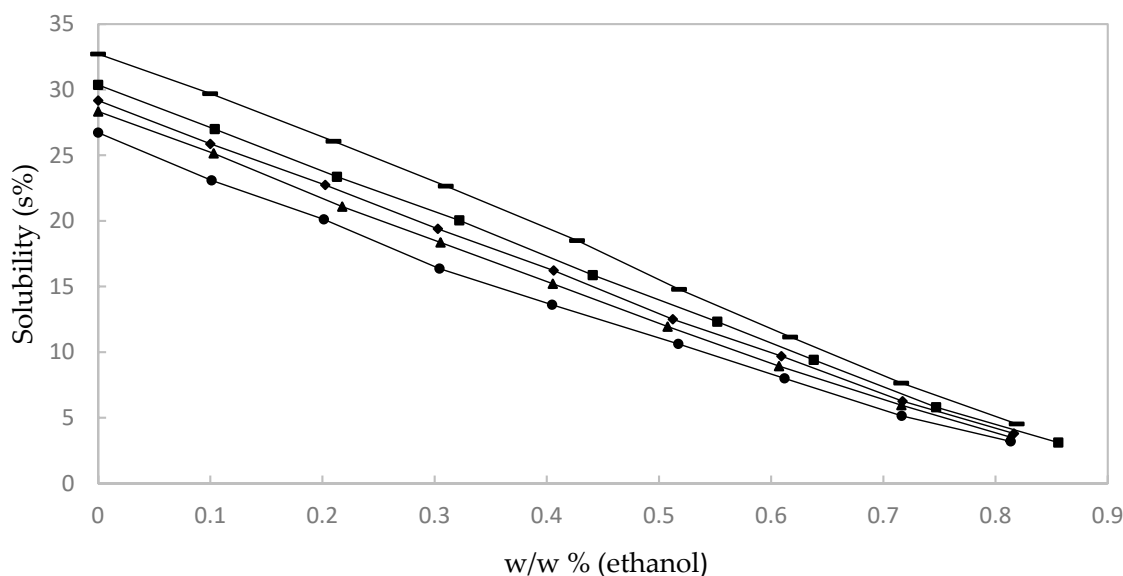

Figure 3. Lithium formate solubility data for the ternary system: 313.15 K –, 303.15 K ■, 298.15 K ♦, 293.15 K ▲, and 283.15 K ●. Data from [29].

4. Results and Discussion

4.1. Lithium Hydroxide

4.1.1. Binary System LiOH + H$_2$O

There are three authors who report activity coefficient data at the same temperature (298.15 K); therefore, it was decided to perform the modeling of the binary system (LiOH + H$_2$O) for the three authors. The data reported by Nasirzadeh et al. [1] have a deviation of 0.00762, the data reported by Robinson and stokes [27] have a deviation of 0.00813, and the data reported by Hammer [28] have a deviation of 0.02158.

After modeling with the modified Pitzer model, it was decided to make a scatter plot to observe the behavior of the data used and ensure that they were consistent. Figures S1–S3 in Supplementary Material present the relative deviation of the values.

The Robinson and Stokes [27] data have a higher dispersion, highlighting that the latter data have a higher error. As for the data of [28], the data have less dispersion than in the previous case; however, as in the case of Nasirzadeh et al. [1] and Robinson, they also have greater uncertainty in the diluted zone.

From the previous results, we have chosen to use the Nasirzadeh et al. [1] data to continue with the modeling of the ternary system due to the better fit obtained in comparison with the other works, and for the fact that the dispersion of his data is more random, while in the other works, there is a certain tendency in the dispersion which makes us think that these data, in addition to the experimental uncertainty, have a systematic error incorporated in their treatment, possibly due to the models or patterns used. Another reason is that Nasirzadeh et al. [1] report data at different temperatures compared to the other two authors.

It is important to note that only α_1 was used for the modeling of the binary system and the comparison of all data; this is because it had already been observed that, with the incorporation of α_2, the improvement in the fit was negligible, which would make the use of α_2 irrelevant for the following calculations.

Table 2 presents the Pitzer parameters determined for the binary system LiOH + H$_2$O; the value of the average absolute deviation (AAD) shows the good agreement between the experimental and calculated values.

Table 2. Parameters of the modified Pitzer model for the binary system LiOH + H$_2$O at 298.15 K.

$\beta_{22}^{(0)}$/kg·mol^{-1}	$\beta_{22}^{(1)}$/kg·mol^{-1}	$\beta_{22}^{(2)}$/kg·mol^{-1}	C_{222}^{γ}/kg^2·mol^{-2}	α_1	α_2	AAD% [a]
0.1523	27.5274	−27.0778	−0.0216	2	1.9345	0.7625

[a] $AAD = \frac{1}{N}\sum_{i=1}^{N}|X_{Exp.i} - X_{Calc.i}|$; N is the number of data used in the regression.

4.1.2. Ternary System LiOH + H$_2$O + C$_2$H$_6$O

Lithium hydroxide crystallizes at 298.15 K with a water molecule, which is why water activity is considered in the modeling. Two additional parameters, B$_{11}$ and C$_{111}$, the second and third coefficients for ethanol, are presented, which were extracted from the work of Galvão et al. [31]. The interaction parameter B$_{11}$ has a value of −0.03411 (kg·mol^{-1}) and the parameter C$_{111}$ has a value of 0.00024 (kg^2·mol^{-2}).

To reach the parameterization, a global objective function is used, which includes the ternary systems and their constituent binary systems over a wide range of temperature and concentration. The objective function used based on the concept of least squares is Equation (13):

$$OF = \frac{\sum\left(\gamma_{i,exp}(x_{exp}) - \gamma_{i,cal}(x_{cal})\right)^2}{n} \tag{13}$$

Table 3 shows the values obtained for the ternary system with their respective average absolute deviation. The AAD value obtained shows the good fit of the solubility data and validates the model for the correlation of these solubility data.

Table 3. Cross-parameters of the modified Pitzer model of the ternary system LiOH + H$_2$O + C$_2$H$_6$O at 298.15 K.

$\beta_{12}^{(0)}$ kg·mol^{-1}	$\beta_{12}^{(1)}$ kg·mol^{-1}	$\beta_{12}^{(2)}$ kg·mol^{-1}	C$_{112}$ kg^2·mol^{-2}	C$_{122}$ kg^2·mol^{-2}	AAD% [a]
−0.5449	8.5285	−3.7190	−0.0188	0.1325	0.5963

[a] $AAD = \frac{1}{N}\sum_{i=1}^{N}\left|X_{Exp.i} - X_{Calc.i}\right|$; N is the number of data used in the regression.

4.2. Lithium Formate

4.2.1. Binary System

The modeling was performed with the data reported by Wood et al. [30], where, initially, the parameters α_1 and α_2 were considered, but the mean absolute deviation did not improve considerably, so it was decided to consider only α_1.

Unfortunately, the data reported by Wood et al. [30] for the activity and osmotic coefficients, being at a very low concentration with respect to the concentration values of the solubility data, have a negative impact on the modeling. Therefore, it was decided to proceed with another modeling procedure for the binary system from its solubility data at different temperatures. The Pitzer parameters of the binary system obtained in the first instance are reported in Table 4, but they are only valid for low concentrations.

Table 4. Parameters of the modified Pitzer model for the binary system CHLiO$_2$ + H$_2$O at 298.15 K, valid up to 0.4 molal.

$\beta_{22}^{(0)}$/kg·mol^{-1}	$\beta_{22}^{(1)}$/kg·mol^{-1}	C_{222}^{γ}/kg^2·mol^{-2}	α_1	AAD% [a]
−0.4735	0.1272	0.5307	2	0.0805

[a] $AAD = \frac{1}{N}\sum_{i=1}^{N}\left|X_{Exp.i} - X_{Calc.i}\right|$; N is the number of data used in the regression.

Parameter Estimation

To model the solubility compositions, the solubility product, Ksp, was determined as a function of temperature through Equation (14), reported by Jiménez et al. [32], where A_i are adjustment parameters and T is the temperature.

$$\mathrm{LogK_{ps}} = A_1 + A_2\mathrm{T} + \frac{A_3}{\mathrm{T}} + A_4\mathrm{Log(T)} + \frac{A_5}{\mathrm{T}^2} \tag{14}$$

The parameters of the activity coefficient model are called the characteristic coefficients of the salt ($\beta_{22}^{(0)}$, $\beta_{22}^{(1)}$, and C_{222}^{ϕ}), the alcohol (B$_{11}$ and C$_{111}$), and the cross-virial coefficients between the salt and the alcohol ($\beta_{12}^{(0)}$, $\beta_{12}^{(1)}$, C$_{112}$, and C$_{122}$). All parameters as a function of temperature were adjusted to the Equation (15), where Q_i are empirical constants, T$_R$ is the reference temperature (298.15 K), and T is the experimental temperature in K.

$$f(T) = Q_1 + Q_2\left(\frac{1}{T} - \frac{1}{T_R}\right) + Q_3 ln\left(\frac{T}{T_R}\right) \tag{15}$$

Table 5 shows the parameters A_i and Q_i obtained for the binary system CHLiO$_2$ and water.

Table 5. A_i (Equation (14)) and Q_i (Equation (15)) values determined for the binary system CHLiO$_2$ + H$_2$O, valid from 283.15 to 313.15 K.

	K$_{sp}$		**Q$_1$**	**Q$_2$**	**Q$_3$**
A$_1$	−0.0002	$\beta_{22}^{(0)}$	0.0022	0.0019	−0.5627
A$_2$	−0.0058	$\beta_{22}^{(1)}$	7.46×10^{-5}	6.47×10^{-5}	−0.0189
A$_3$	-8.13×10^{-5}	C_{222}^{γ}	0.0095	0.0114	6.51×10^{-5}

Although this procedure is valid and was necessary to perform due to the scarcity of reported data from the lithium format, it is recommended to integrae the activity or osmotic coefficient data of the binary system to the procedure, and thus determine together the parameters, which would be much more consistent when considering these thermodynamic properties and the solubility product.

4.2.2. Ternary System $CHLiO_2$ + H_2O + C_2H_6O

To determine the Debye–Hückel constants (A and b), data reported by Zafarani-Moattar and Majdan-Cegincara [23] for ethanol density and data reported by Åkerlöf [24] for the dielectric constant for ethanol, at five different temperatures, were used (Table S1). These data were fitted to an equation to determine the value at the study temperature. The figures can be found in Supplementary Material (Figures S4 and S5).

Lithium formate crystallizes with a water molecule up to 364.15 K, so the parameters B_{11} and C_{111} are included in the modeling; however, unlike lithium hydroxide, in this case we worked with five different temperatures, so these parameters must be a function of temperature, as described in Equation (15); these parameters have already been reported by Galvão et al. [31].

Table 6 shows the results obtained for the Pitzer parameters at each temperature for the ternary system $CHLiO_2$ + H_2O + C_2H_6O and the solubility product values.

Table 6. Cross-parameters of the modified Pitzer model of the ternary system $CHLiO_2$ + H_2O + C_2H_6O at different temperatures and solubility products, K_{sp}.

T/K	$\beta_{12}^{(0)}$ kg·mol^{-1}	$\beta_{12}^{(1)}$ kg·mol^{-1}	C_{112} kg^2·mol^{-2}	C_{122} kg^2·mol^{-2}	K_{sp}	AAD% [a]
283.15	−0.3167	1.3382	−0.0018	0.0461	0.0225	0.2821
293.15	−0.2494	−2.1863	0.0055	0.0332	0.0197	0.1620
298.15	−0.2135	0.7527	−0.0007	0.0297	0.0184	0.1584
303.15	−0.2527	0.4829	0.0002	0.0295	0.0172	0.1653
313.15	−0.1299	−1.2661	0.0025	0.0168	0.0150	0.2113

[a] $AAD = \frac{1}{N}\sum_{i=1}^{N}|X_{Exp.i} - X_{Calc.i}|$; N is the number of data used in the regression.

4.3. Precipitate Calculation

Quantifying the amount of precipitated salt (or supersaturation) for different percentages of antisolvent in the system is crucial information for the process design. This calculation can be performed starting from an initial equilibrium condition, in which the salt is saturated in water; if any amount of antisolvent (ethanol) is added to this system, precipitation occurs, followed by the establishment of a new equilibrium condition in which the salt will be saturated again, but now in a new water + antisolvent medium.

Galvão et al. [31] have developed an equation from Equation (1) incorporating this new equilibrium condition, as shown in Equation (16), where *P* corresponds to the precipitate in mole fraction, X_0 is the initial salt mole fraction in the saturated solution, and *a* corresponds to the activity of water in solution.

$$P^2 - 2X_0 + X_0^2 - \frac{K_{sp}}{\left(\gamma_\pm^2 * a\right)} = 0 \tag{16}$$

4.3.1. Lithium Hydroxide

Table 7 shows the amount of lithium hydroxide precipitated and the yield of the process as a function of the ethanol concentration. The highest yield was obtained with a concentration of 56.49% ethanol, where 93.8 g LiOH/kg ethanol was obtained. The yield is only 9%, so, in contrast to other antisolvents studied, ethanol could not be the best choice for use in the drowning-out crystallization process.

Table 7. Solubility product, K_{sp}, the initial solubility, X_0, the water activity, a, the amount of LiOH precipitate, P, in mole fraction and g/kg solv. as a function of the ethanol weight percentage, and the yield (Y) of the process at 298.15 K.

K_{sp}	X_0	a	P (frac. Mol)	P (g/kg solv)	*w/w* % Ethanol	Y%
0.0037	0.0853	0.9322	0.0000	0.0000	0.00	0.00
		0.8140	0.0158	37.2295	9.94	3.72
		0.7685	0.0284	61.5564	19.97	6.16
		0.7478	0.0339	68.4350	28.52	6.84
		0.7296	0.0436	79.7250	40.07	7.97
		0.7447	0.0482	82.3849	47.37	8.24
		0.8273	0.0510	80.1891	56.50	8.02
		0.8167	0.0600	93.8761	56.49	9.39
		0.8875	0.0586	88.6288	60.05	8.86

4.3.2. Lithium Formate

The values of the precipitate as a function of the ethanol concentration and the results at the five temperatures are presented in Supplementary Material (Tables S2–S6). The results obtained are plotted to analyze the effect of temperature, which can be seen in Figure 4.
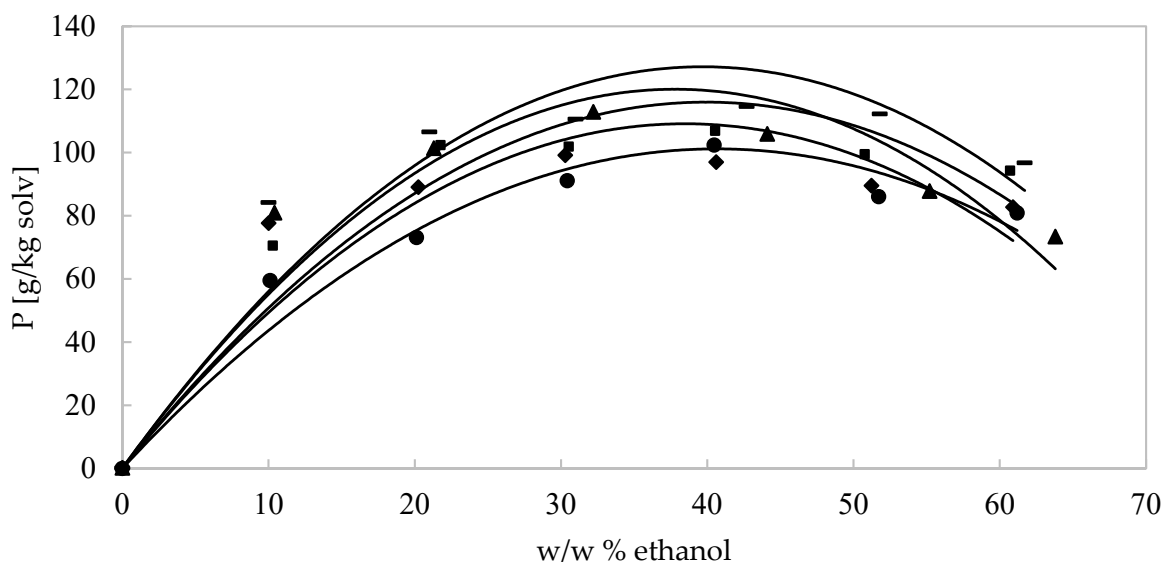

Figure 4. Comparison of lithium formate precipitate results at different temperatures: 283.15 K ●, 293.15 K ■, 298.15 K ♦, 303.15 K ▲, and 313.15 K ▬. Curves are guides for the eye.

The precipitate increases with temperature, which is to be expected, since the solubility increases with temperature; however, it can be seen that the trend line at 293.15 K is above the trend line at 298.15 K, which could be due to the experimental uncertainty of the data used. It is observed that the solubility data at 293.15 K are very close to those at 298.15 K; practically, some points would be in the margin of the experimental uncertainty. This undoubtedly has repercussions on the results of the modeling.

Regarding the amount of ethanol to be added to obtain the optimum amount of precipitate in each case, it can be observed that, as the temperature increases, this amount decreases, since, at 283.15 K, 40% by weight of ethanol is the optimum amount and at 313.15 K, the optimum amount is 36%; these results make sense because, as the temperature is higher, it is not necessary to add more ethanol to obtain the desired precipitate, since the temperature is a factor that affects the solubility of the salts.

4.4. Drowning-Out Crystallization Process

4.4.1. Lithium Hydroxide

The design of the drowning-out crystallization process consists of three pieces of equipment, a crystallizer, a filter or centrifuge, and a dryer working at 100 °C, in which lithium hydroxide monohydrate crystals are obtained. Figure S6 in Supplementary Material shows the flow diagram with the respective currents. It was decided to use this process design due to the results obtained from the article by Justel et al. [33], in which three options of the crystallization process designs are presented. Of these three options, the third one (which is the one presented in this work) was the best evaluated because it obtained the lowest energy consumption and the highest production.

The mass and energy balance are presented in Table 8, where the enthalpy values for each stream are negative; so, it is determined that they correspond to heat flows, which should be removed for the process to occur. The energy balance for each equipment is: crystallizer, 0 MJ/kg·s; filter, 0.2 MJ/kg·s; dryer, 3.07 MJ/kg·s.

Table 8. Mass and energy balance for the drowning-out crystallization process of lithium hydroxide.

		Flows		*w/w* %			Total H
Stream	T/K	kg/s	$LiOH \cdot H_2O$	Ethanol	LiOH	Water	MJ/kg·s
1	298.15	100.0000	0.0000	0.0000	0.1278	0.8722	−1655.12
2	298.15	93.0097	0.0000	1.0000	0.0000	0.0000	−579.90
3	298.15	15.5717	14.8302	0.0000	0.5710	0.4290	−288.83
4	298.15	177.4379	0.0000	0.5220	0.0242	0.4538	−1954.32
5	298.15	15.1268	14.8302	0.5220	0.0242	0.4538	−283.75
6	298.15	0.4449	0.0000	0.5220	0.0242	0.4538	−4.88
7	373.15	14.8401	14.8401	0.0000	0.0000	0.0000	−277.93
8	373.15	0.2867	0.0000	0.5220	0.0242	0.4538	−2.76

4.4.2. Lithium Formate

The design of the drowning-out crystallization process for lithium formate is the same as for lithium hydroxide. The mass and energy balance were only calculated at 298.15 K in order to make a comparison between the two salts; however, since lithium formate crystallizes with a water molecule up to 364.15 K, the dryer was operated at that temperature. The results can be seen in Table 9, and the energy balance for each equipment is: the crystallizer, 0 MJ/kg·s; filter, 0 MJ/kg·s; dryer, 2.03 MJ/kg·s.

Table 9. Mass and energy balance for the lithium formate drowning-out crystallization process.

		Flows		*w/w* %			Total H
Stream	T/K	kg/s	$CHLiO_2 \cdot H_2O$	Ethanol	$CHLiO_2$	Water	MJ/kg·s
1	298.15	100.0000	0.0000	0.0000	0.2920	0.7080	−1519.40
2	298.15	46.1320	0.0000	1.0000	0.0000	0.0000	−287.63
3	298.15	27.6230	26.3080	0.0000	0.7430	0.2570	−388.14
4	298.15	118.5090	0.0000	0.3850	0.0800	0.5350	−1434.64
5	298.15	26.8340	26.3080	0.3850	0.0800	0.5350	−378.69
6	298.15	0.2630	0.0000	0.3850	0.0800	0.5350	−9.45
7	364.15	26.3650	26.3650	0.0000	0.0000	0.0000	−371.32
8	364.15	0.4690	0.0000	0.3850	0.0800	0.5350	−5.34

5. Conclusions

- A comprehensive compilation of bibliographic data for lithium hydroxide and lithium formate, including the activity, osmotic, and solubility coefficients, was undertaken from various authors. The analysis for lithium hydroxide involved assessing the activity coefficient data from different sources to identify the most suitable for modeling,

with the conclusion highlighting the necessity for a more thorough examination of these experimental data. In contrast, for lithium formate, a similar analysis could not be conducted due to the limited and generally sparse information available in the literature.

- The application of the modified Pitzer model to model the thermodynamic properties was successful for both salts, involving parameterization for both binary and ternary systems, with an average standard deviation of less than 1%. However, limitations arose due to the limited data available in the literature. In particular, for lithium formate in the ternary system, determining the solubility product required the use of an alternative procedure.

- The examination of the temperature and antisolvent (ethanol) in the ternary system of lithium formate revealed that higher temperatures lead to an increased precipitate yield, aligning with expectations. The study also identified the optimal amount of antisolvent to achieve the highest process yield. In the design of the crystallization process using the drowning method, for both lithium hydroxide and lithium formate, three stages were considered: the crystallizer, filter, and dryer. This approach is advantageous, as it eliminates the need for mixing or recrystallization stages, resulting in significant energy savings.

Supplementary Materials: The following supporting information can be downloaded at: https://www.mdpi.com/article/10.3390/met14010078/s1, Figure S1: Relative deviation between experimental and calculated values of the activity coefficient at 298.15 K from the data of [1]. The horizontal lines correspond to the average relative deviations of the fit; Figure S2: Relative deviation between experimental and calculated values of the activity coefficient at $298.15°$ K from the data of [27]. The horizontal lines correspond to the average relative deviations of the fit; Figure S3: Relative deviation between experimental and calculated values of the activity coefficient at $298.15°$ K from the data of [28]. The horizontal lines correspond to the average relative deviations of the fit; Figure S4: Density at different temperatures; Figure S5: Dielectric constant at different temperatures; Figure S6: Drowning-out crystallization process of LiOH at 298.15 K; Table S1: Density and dielectric constant data of ethanol at different temperatures; Table S2: Solubility product, Kps, initial solubility, X0, water activity, a, amount of $CHLiO_2$ precipitate in mole fraction and g/kg solv, as a function of ethanol weight percentage, and yield (Y) of the process at 283.15 K; Table S3: Solubility product, Kps, initial solubility, X0, water activity, a, amount of $CHLiO_2$ precipitate in mole fraction and g/kg solv, as a function of ethanol weight percentage, and yield (Y) of the process at 293.15 K; Table S4: Solubility product, Kps, initial solubility, X0, water activity, a, amount of $CHLiO_2$ precipitate in mole fraction and g/kg solv, as a function of ethanol weight percentage, and yield (Y) of the process at 298.15 K; Table S5: Solubility product, Kps, initial solubility, X_0, water activity, a, amount of $CHLiO_2$ precipitate in mole fraction and g/kg solv, as a function of ethanol weight percentage, and yield (Y) of the process at 303.15 K; Table S6: Solubility product, Kps, initial solubility, X0, water activity, a, amount of $CHLiO_2$ precipitate in mole fraction and g/kg solv, as a function of ethanol weight percentage, and yield (Y) of the process at 313.15 K.

Author Contributions: Conceptualization, Y.P.J.; Methodology, R.G.; Validation, Y.B.; Formal analysis, Y.P.J.; Investigation, R.G. and Y.P.J.; Writing—original draft, R.G. and Y.B.; Writing—review and editing, Y.B.; Supervision, Y.P.J. All authors have read and agreed to the published version of the manuscript.

Funding: The APC was funded by the Universidad de Antofagasta and SMI-ICE-Chile.

Data Availability Statement: The data presented in this study are openly available in ACS Publication, Industrial & Engineering Chemistry Research at [https://doi.org/10.1021/IE0489148]; Royal Society of Chemistry [https://doi.org/10.1039/TF9494500612]; AIP Publishing, Journal of Physical and Chemical Reference Data [https://doi.org/10.1063/1.3253108].

Acknowledgments: R. González and Y. Jimenez would like to thank the Department of Chemical Engineering and Mineral Processes of the Universidad de Antofagasta for making this work possible. Y. Barrueto would like to thank the Universidad Técnica Federico Santa María and SMI-ICE-Chile for the support provided.

Conflicts of Interest: The authors declare no conflict of interest.

References

1. Nasirzadeh, K.; Neueder, R.; Kunz, W. Vapor Pressures and Osmotic Coefficients of Aqueous LiOH Solutions at Temperatures Ranging from 298.15 to 363.15 K. *Ind. Eng. Chem. Res.* **2005**, *44*, 3807–3814. [CrossRef]
2. Zhao, L.-M.; Chen, Q.-B.; Ji, Z.-Y.; Liu, J.; Zhao, Y.-Y.; Guo, X.-F.; Yuan, J.-S. Separating and recovering lithium from brines using selective-electrodialysis: Sensitivity to temperature. *Chem. Eng. Res. Des.* **2018**, *140*, 116–127. [CrossRef]
3. Keller, A.; Sterner, P.; Hlawitschka, M.; Bart, H.-J. Extraction kinetics of cobalt and manganese with D2EHPA from lithium-ion battery recyclate. *Chem. Eng. Res. Des.* **2022**, *179*, 16–26. [CrossRef]
4. Pu, S.; Hadinoto, K. Continuous crystallization as a downstream processing step of pharmaceutical proteins: A review. *Chem. Eng. Res. Des.* **2020**, *160*, 89–104. [CrossRef]
5. Takiyama, H. Morphology of NaCl Crystals in Drowning-Out Precipitation Operation. *Chem. Eng. Res. Des.* **1998**, *76*, 809–814. [CrossRef]
6. Ortiz, C.P.; Cardenas-Torres, R.E.; Martínez, F.; Delgado, D.R. Solubility of Sulfamethazine in the Binary Mixture of Acetonitrile + Methanol from 278.15 to 318.15 K: Measurement, Dissolution Thermodynamics, Preferential Solvation, and Correlation. *Molecules* **2021**, *26*, 7588. [CrossRef] [PubMed]
7. Pina, C.M.; Fernández-Díaz, L.; Prieto, M.; Veintemillas-Verdaguer, S. Metastability in drowning-out crystallisation: Precipitation of highly soluble sulphates. *J. Cryst. Growth* **2001**, *222*, 317–327. [CrossRef]
8. Pitzer, K.S. Thermodynamics of electrolytes. I. Theoretical basis and general equations. *J. Phys. Chem.* **1973**, *77*, 268–277. [CrossRef]
9. Fuentes, A.; Casas, J.M. Modelling of ionic conductivity in nitrate brines to estimate solute concentrations. *Hydrometallurgy* **2021**, *203*, 105639. [CrossRef]
10. Fuentes, A.N.; Justel, F.J.; Jimenez, Y.P.; Casas, J.M. Speciation and thermochemical modeling of the ternary system $CuSO_4$–H_2SO_4–H_2O in the temperature range 273.15–373.15 K. *J. Mol. Liq.* **2023**, *391*, 123377. [CrossRef]
11. Li, D.; Meng, L.; Guo, Y.; Deng, T.; Yang, L. Chemical engineering process simulation of brines using phase diagram and Pitzer model of the system $CaCl_2SrCl_2H_2O$. *Fluid Phase Equilibria* **2019**, *484*, 232–238. [CrossRef]
12. Wu, Y.T.; Lin, D.Q.; Zhu, Z.Q.; Mei, L.H. Prediction of liquid-liquid equilibria of polymer salt aqueous two-phase systems by a modified Pitzer's virial equation. *Fluid Phase Equilibria* **1996**, *124*, 67–79. [CrossRef]
13. Lovera, J.A.; Padilla, A.P.; Galleguillos, H.R. Correlation of the solubilities of alkali chlorides in mixed solvents: Polyethylene glycol + H_2O and Ethanol + H_2O. *Calphad* **2012**, *38*, 35–42. [CrossRef]
14. Villca, G.; Justel, F.J.; Jimenez, Y.P. Water activity, density, sound velocity, refractive index and viscosity of the {$(NH_4)_6Mo_7O_{24}$ + poly(ethylene glycol) + H_2O} system in the temperature range from 313.15 to 333.15 K: Experiment and modelling. *J. Chem. Thermodyn.* **2020**, *142*, 105986. [CrossRef]
15. Deyhimi, F.; Abedi, M. NaCl + CH_3OH + H_2O mixture: Investigation using the pitzer and the modified pitzer approaches to describe the binary and ternary ion-nonelectrolyte interactions. *J. Chem. Eng. Data* **2012**, *57*, 324–329. [CrossRef]
16. Ma, L.; Li, S.; Zhai, Q.; Jiang, Y.; Hu, M. Thermodynamic study of RbF/CsF in amino acid aqueous solution based on the pitzer, modified pitzer, and extended debye-Hückel models at 298.15 K by a potentiometric method. *Ind. Eng. Chem. Res.* **2013**, *52*, 11767–11772. [CrossRef]
17. Pramanik, S.; Das, B. Osmotic and Activity Coefficients of Lithium Nitrate in Ethanol under High Pressures. *J. Solut. Chem.* **2022**, *51*, 1589–1602. [CrossRef]
18. Yuan, F.; Li, L.; Guo, Y.; Deng, T. Dilution enthalpies of $LiBO_2$ and LiB_5O_8 aqueous solutions at 298.15 K and the application of ion-interaction model. *Thermochim. Acta* **2020**, *685*, 178506. [CrossRef]
19. Taboada, M.E.; Graber, T.A.; Cisternas, L.A.; Cheng, Y.S.; Ng, K.M. Process Design for Drowning-Out Crystallization of Lithium Hydroxide Monohydrate. *Chem. Eng. Res. Des.* **2007**, *85*, 1325–1330. [CrossRef]
20. Graber, T.A.; Morales, J.W.; Robles, P.A.; Galleguillos, H.R.; Taboada, M.E. Behavior of $LiOH·H_2O$ crystals obtained by evaporation and by drowning out. *Cryst. Res. Technol.* **2008**, *43*, 616–625. [CrossRef]
21. Kell, G.S. Density, Thermal Expansivity, and Compressibility of Liquid Water from 0° to 150 °C: Correlations and Tables for Atmospheric Pressure and Saturation Reviewed and Expressed on 1968 Temperature Scale. *J. Chem. Eng. Data* **1975**, *20*, 97–105. [CrossRef]
22. Malmberg, C.G.; Maryott, A.A. Dielectric Constant of Water from 0° to 100 °C. *J. Res. Natl. Bur. Stand. (1934)* **1956**, *56*. Available online: https://books.google.com.mx/books?hl=es&lr=&id=i1IXAQAAMAAJ&oi=fnd&pg=PP11&dq=C.G.+Malmberg,+A.A.+Maryott,+Dielectric+constant+of+water+from+0+to+100+C,+J.+Res.+Natl.+Bur.+Stand.+56+(1956)+(1934)+1&ots=6PETbSOyec&sig=cHC-5usSaoCynZ1-dSa6-zu-IMY#v=onepage&q&f=false (accessed on 8 December 2022). [CrossRef]
23. Zafarani-Moattar, M.T.; Majdan-Cegincara, R. Density, Speed of Sound, and Viscosity of Binary Mixtures of Poly(propylene glycol) 400 + Ethanol and + 2-Propanol at Different Temperatures. *J. Chem. Eng. Data* **2008**, *53*, 2211–2216. [CrossRef]
24. Åkerlöf, G.; Turck, H.E. The Solubility of Some Strong, Highly Soluble Electrolytes in Methyl Alcohol and Hydrogen Peroxide-Water Mixtures at 25°. *J. Am. Chem. Soc.* **1935**, *57*, 1746–1750. [CrossRef]
25. Taboada, M.E.; Véliz, D.M.; Galleguillos, H.B.; Graber, T.A. Solubility, Density, Viscosity, Electrical Conductivity, and Refractive Index of Saturated Solutions of Lithium Hydroxide in Water + Ethanol. *J. Chem. Eng. Data* **2004**, *50*, 187–190. [CrossRef]

26. Taboada, M.E.; Galleguillos, H.R.; Graber, T.A.; Álvarez-Benedí, J. Density, viscosity, refractive index and electrical conductivity of saturated solutions of the lithium hydroxide + etanol + water system at 298.15 K, and thermodynamic description of the solid–liquid equilibrium. *Fluid Phase Equilibria* **2005**, *235*, 104–111. [CrossRef]
27. Robinson, R.A.; Stokes, R.H. Tables of osmotic and activity coefficients of electrolytes in aqueous solution at 25 °C. *Trans. Faraday Soc.* **1949**, *45*, 612–624. [CrossRef]
28. Hamer, W.J.; Wu, Y.-C. Osmotic Coefficients and Mean Activity Coefficients of Uni-univalent Electrolytes in Water at 25 °C. *J. Phys. Chem. Ref. Data* **2009**, *1*, 1047. [CrossRef]
29. Cartón, A.; Sobrón, F.; de La Fuente, M.; de Blas, E. Composition, Density, Viscosity, Electrical Conductivity, and Refractive Index of Saturated Solutions of Lithium Formate + Water + Ethanol. *J. Chem. Eng. Data* **1996**, *41*, 74–78. [CrossRef]
30. Wood, R.H.; Wicker, R.K.; Kreis, R.W. Freezing points, osmotic coefficients, and activity coefficients of salts in N-Methylacetamide. I. Alkali halides and nitrates. *J. Phys. Chem.* **1971**, *75*, 2313–2318. [CrossRef]
31. Galvão, A.C.; Jiménez, Y.P.; Justel, F.J.; Robazza, W.S.; Feyh, J.V.T. Modeling of the solid-liquid equilibrium of NaCl, KCl and NH$_4$Cl in mixtures of water and ethanol by the modified Pitzer model. *J. Mol. Liq.* **2021**, *322*, 114968. [CrossRef]
32. Jimenez, Y.P.; Justel, F.; Casas, J.M. Model of speciation and solubility of sodium molybdate in water, 0–110 °C. *J. Mol. Liq.* **2022**, *346*, 117096. [CrossRef]
33. Justel, F.J.; Taboada, M.E.; Jiménez, Y.P.; Graber, T.A. Process Design to Obtain Copper Sulfate Crystals Using Solid–Liquid Equilibrium of Copper Sulfate–Sulfuric Acid–Seawater. *J. Sustain. Metall.* **2021**, *7*, 192–202. [CrossRef]